Inhibition of Lysyl Oxidase with β-aminopropionitrile Improves Venous Adaptation after Arteriovenous Fistula Creation

Diana R. Hernandez,[1] Brandon Applewhite,[1,2] Laisel Martinez,[1] Tyler Laurito,[2] Marwan Tabbara,[1] Miguel G. Rojas,[1] Yuntao Wei,[1] Guillermo Selman,[3] Marina Knysheva,[4] Omaida C. Velazquez,[1] Loay H. Salman,[3] Fotios M. Andreopoulos,[2] Yan-Ting Shiu,[4] and Roberto I. Vazquez-Padron [1]

Abstract

Background The arteriovenous fistula (AVF) is the preferred hemodialysis access for patients with ESKD. Yet, establishment of a functional AVF presents a challenge, even for the most experienced surgeons, because postoperative stenosis frequently occludes the AVF. Stenosis results from the loss of compliance in fibrotic areas of the fistula, which turns intimal hyperplasia into an occlusive feature. Fibrotic remodeling depends on deposition and crosslinking of collagen by lysyl oxidase (LOX), an enzyme that catalyzes the deamination of lysine and hydroxylysine residues, facilitating intra/intermolecular covalent bonds. We postulate that pharmacologic inhibition of LOX increases postoperative venous compliance and prevents stenosis in a rat AVF model.

Methods LOX gene expression and vascular localization were assayed in rat AVFs and human preaccess veins, respectively. Collagen crosslinking was measured in humans AVFs that matured or failed, and in rat AVFs treated with β-aminopropionitrile (BAPN), an irreversible LOX inhibitor. BAPN was either injected systemically or delivered locally around rat AVFs using nanofiber scaffolds. The major endpoints were AVF blood flow, wall fibrosis, collagen crosslinking, and vascular distensibility.

Results Nonmaturation of human AVFs was associated with higher LOX deposition in preaccess veins ($n=20$, $P=0.03$), and increased trivalent crosslinks ($n=18$, $P=0.03$) in human AVF tissues. Systemic and local inhibition of LOX increased AVF distensibility, while reducing wall fibrosis and collagen crosslinking in rat fistulas.

Conclusions Our results demonstrate that BAPN-mediated inhibition of LOX significantly improves vascular remodeling in experimental fistulas.

KIDNEY360 2: 270–278, 2021. doi: https://doi.org/10.34067/KID.0005012020

Introduction

A functional hemodialysis access is the lifeline for approximately 500,000 patients with ESKD in the United States (1). The preferred access, the arteriovenous fistula (AVF), created by vein-to-artery anastomosis in the arm (2), incites a complex biological transformation that should yield a superficial vessel with a thickened wall and increased luminal area capable of supporting blood flow over 600 ml/min after maturation (3). However, postoperative venous stenosis stymies maturation, increasing patient morbidity (thrombosis, revision, new AVF) and health care costs (4). AVF failure rates have remained unacceptably high (approximately 40%) for decades (4), due in large part to the scarce knowledge on the mechanisms underlying AVF stenosis.

The biological processes leading to the formation and progression of stenotic lesions in AVFs have only begun to be elucidated. We have recently disclosed a link between postoperative fibrosis and nonmaturation, especially when combined with intimal hyperplasia (5). The circumferential orientation of collagen fibers around the lumen is also predictive of nonmaturation, suggesting that not only the degree but the quality of medial fibrosis plays a role in venous remodeling (5). Whether the biomechanical characteristics of postoperative fibrosis determines venous compliance after fistula creation remains unknown.

Lysyl oxidase (LOX) catalyzes the deamination of lysine and hydroxylysine residues, facilitating intra/intermolecular covalent crosslinking (6). Collagen and elastin, the main substrates of LOX, likely govern vascular mechanical properties after fistula creation (7). In the case of collagen, LOX forms divalent (immature) crosslinks between two adjacent triple-helices, and indirectly promotes the spontaneous (mature)

[1]DeWitt Daughtry Family Department of Surgery, Division of Vascular Surgery, Leonard M. Miller School of Medicine, University of Miami, Miami, Florida
[2]Department of Biomedical Engineering, College of Engineering, University of Miami, Coral Gables, Florida
[3]Division of Nephrology and Hypertension, Albany Medical College, Albany, New York
[4]Division of Nephrology and Hypertension, University of Utah, Salt Lake City, Utah

Correspondence: Roberto I. Vazquez-Padron, DeWitt Daughtry Family Department of Surgery, Leonard M. Miller School of Medicine, University of Miami, 1600 NW, 10th Avenue, RMSB room 1048, Miami, FL 33136. Email: rvazquez@med.miami.edu

crosslinking with a third triple helix (8). Collagen tensile strength relies on LOX-mediated crosslinking (9). Hyperactive LOX is associated with hypoxia-induced metastasis (10,11), myocardial fibrosis (12), and pulmonary hypertension (13). LOX inhibition has been proposed as a pharmacologic approach to treat fibrosis (7). However, it is unknown whether dysregulated LOX activity leads to stenosis in failed AVFs. We hypothesize that systemic and local inhibition of LOX with β-aminopropionitrile (BAPN), a naturally occurring LOX inhibitor, promotes adaptive remodeling in experimental AVFs by reducing collagen crosslinking. Systemic administration of BAPN has dose-limiting side effects in humans (*i.e.*, lathyrism) (14,15). Therefore, a local delivery method will be tested to achieve high drug concentrations in the fistula with minimal systemic toxicity.

Materials and Methods

Detailed experimental methods are provided in the Supplemental Materials and Methods along with their corresponding Supplemental References.

Human Veins and AVFs

Paraffin-embedded cross-sections of preaccess veins (*n*=20, ten matured and ten failed after AVF creation) from patients who received a planned two-stage upper arm AVF at Jackson Memorial Hospital or the University of Miami were randomly selected from the University of Miami Vascular Biobank. In addition, 18 independent AVF specimens (eight matured and ten failed) preserved in *RNAlater* (Qiagen) and collected at the time of second-stage surgery were randomly obtained from the biorepository. The study was performed according to the ethical principles of the Declaration of Helsinki and regulatory requirements at both institutions. The ethics committee and Institutional Review Board at the University of Miami approved the study.

Rat Model of AVF Maturation

Sprague Dawley rats (280–320 g) were purchased from Envigo (Indianapolis, IN). AVFs were created by an end-to-side anastomosis of the epigastric vein to the nearby femoral artery (16). In total, 96 rats of both sexes were randomly allocated to experimental groups for molecular analysis (*n*=18), systemic BAPN and vehicle administration (*n*=42), and local drug delivery (*n*=36).

Scaffold Fabrication and Characterization

Scaffolds were fabricated using an electrospinning apparatus.

Mass Spectrometry

Cumulative BAPN release was quantified with a direct infusion/triple quadrupole mass spectrometer (17) configured in positive mode, 42 eV collision energy (10,000–150,000 m/z) scan range, and parent-ion scan mode. Immature (hydroxylysinonorleucine and dihydroxylysinonorleucine) and mature crosslinks (pyridinoline and deoxypyridinoline) were quantified in the venous limb of AVFs as previously described (18).

Pressure Myography

The proximal and distal venous segments of the AVF were placed on a pair of steel cannulas of a pressure myograph system, DMT Model 110P (Danish Myo Technology, Ann Arbor, MI) and secured with surgical nylon sutures. The circumferential wall strain and stress and incremental elastic modulus (E_{inc}) were calculated as previously described (19).

Immunohistochemistry

Paraffin-embedded rat AVFs were stained with Masson's trichrome to quantify wall fibrosis. Vascular LOX and elastin were detected in paraffin embedded venous cross-sections with polyclonal antibodies.

Gene Expression

Total RNA was isolated from the venous limb of AVFs and reverse transcribed as previously described (20). Changes in gene expression were assessed using Taq-Man Gene Expression Assays (Applied Biosystems, Waltham, MA).

Statistical Analyses

Statistical analyses were performed using GraphPad Prism version 8 for Windows (GraphPad Software, San Diego, CA). Normally distributed data were compared using unpaired *t* tests with Welch's correction and expressed as mean±SD (or mean±SEM where indicated in figures). Non-normally distributed data were compared using the Mann–Whitney *U* test and expressed as median and interquartile range (IQR). A *P* value <0.05 was considered significant.

Results

Increased Collagen Crosslinking in Human AVFs that Failed

We first evaluated the vascular expression of LOX in 20 randomly selected human preaccess veins used for two-stage upper arm AVF creation by immunohistochemistry. Half of the veins matured, whereas the remaining ten failed to mature after AVF creation. Veins that failed had higher accumulation of LOX in the wall (% LOX$^+$ area) than those that matured successfully (median 5.30; IQR, 3.63–10.32 versus 1.69; IQR, 0.69–5.04, *P*=0.03; Figure 1, A and B).

We then quantified collagen crosslinking in AVF tissues collected from an independent group of patients (*n*=18) at the time of second-stage surgery. Eight of these AVFs matured and underwent a standard transposition for superficialization during the second-stage procedure, whereas ten AVFs failed and required a short transposition, ligation, or arteriovenous graft extension. The time from AVF creation to postoperative sample collection was similar between AVFs that matured or failed (mean 74.4±SD 27.1 versus 66.7±28.5 days, respectively; *P*=0.57). AVFs that failed had significantly higher mature crosslinking density than those that matured (0.061 μmol/mg of dry weight; IQR, 0.039–0.089 versus 0.041; IQR, 0.025–0.045, *P*=0.03), and a trend toward increased immature density (1.29±0.56 nmol/mg of dry weight in AVFs that failed versus 0.87±0.29 in those that matured, *P*=0.06; Figure 1, C and D). These results support the hypothesis that increased LOX
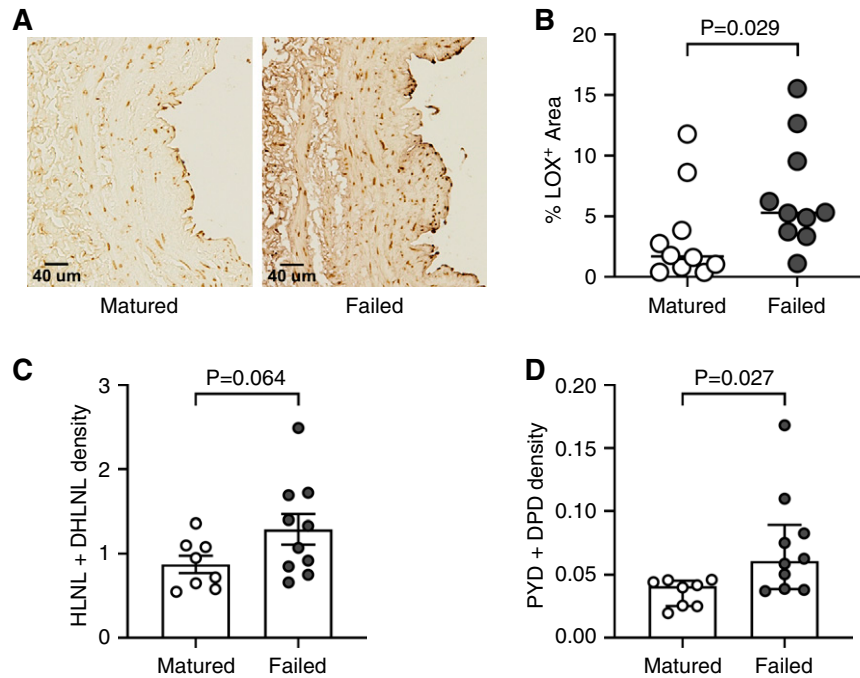
Figure 1. | Increased lysyl oxidase (LOX) deposition and collagen crosslinking are associated with nonmaturation of human arteriovenous fistulas (AVFs). (A) Representative anti-LOX immunohistochemistry in preaccess upper arm veins that matured or failed after AVF creation. (B) Quantification of the LOX-positive wall area in cross-sections of preaccess veins that matured ($n=10$) or failed ($n=10$). (C and D) Immature (C) and mature (D) crosslinking density in human upper arm AVF tissues that matured ($n=8$) or failed ($n=10$), collected at the time of second-stage transposition surgery. Divalent immature crosslinks hydroxylysinonorleucine (HLNL) and dihydroxylysinonorleucine (DHLNL), and trivalent mature crosslinks pyridinoline (PYD) and deoxypyridinoline (DPD) were quantified by ultra-performance liquid chromatography-electrospray ionization-tandem mass spectrometry (UPLC-ESI-MS/MS). Immature crosslinking density is expressed as nmol per mg of dry weight of tissue, whereas mature density is presented as μmol per mg of dry weight.

activity during AVF remodeling is associated with access failure.

AVF Creation Affects Expression of Extracellular Matrix Genes

The rodent AVF model enables mechanistic studies of AVF remodeling (16). We utilized a rat AVF model to examine the postoperative changes in mRNA expression of *Lox* and *Lox*-like (*LoxL*) genes. *Lox* mRNA was significantly upregulated 5 days postsurgery compared with the expression in the vein at the time of AVF creation (fold change 2.81 ± 0.92 over baseline, $P=0.005$; Figure 2). The AVF portrayed pronounced wall thickening at 20 days after surgery (Supplemental Figure 1A), representing the adaptation of the vein to arterial circulation. LOX accumulated in cells of the media and adventitia at this time point after AVF creation (Supplemental Figure 1B).

We then analyzed the mRNA expression pattern of extracellular matrix (ECM) genes and remodeling factors after AVF surgery (Supplemental Figure 2). Matrix metalloproteases (MMP), fibronectin, elastin, and collagens were upregulated after surgery. MMP-2 and MMP-9 were upregulated 2.3- and 300-fold, respectively, at postoperative day 5. The alpha 1 chains of collagens type I and III had an increase in expression that peaked at day 5, whereas elastin increased linearly over 33 days. These findings establish a temporal framework for LOX-targeted interventions.

Systemic BAPN Improves AVF Remodeling in Rats

We tested whether inhibition of LOX improved vessel remodeling and AVF outcomes at 21 days postsurgery in the rat model. Systemic inhibition of LOX using BAPN improved blood flow compared with vehicle controls (23.40 ± 10.50 versus 10.33 ± 4.27 ml/min, $P=0.05$) (Figure 3A), and significantly reduced fibrosis (as percent of wall area) in the AVF wall (10.42 ± 3.38 versus $23.72\pm11.88\%$, $P=0.01$; Figure 3, B and C, Supplemental Figure 3A). BAPN treatment reduced immature collagen crosslinking compared with vehicle controls (0.42 ± 0.12 versus 1.19 ± 0.33 μmol/mg of dry weight, $P=0.002$; Figure 3D), and showed a trend toward decreasing mature crosslinking (0.10 ± 0.03 versus 0.21 ± 0.15 μmol/mg of dry weight, $P=0.12$; Figure 3E). Interestingly, systemic inhibition of LOX decreased wall thickness in the fistula compared with the vehicle control (Supplemental Figure 3B), suggesting an effect on smooth muscle cell proliferation and/or migration. However, in contrast to the reduction of wall fibrosis (Figure 3C), the treatment had no effect on elastin content (Supplemental Figure 4, A and B). Treated AVFs also had more distensibility (percent deformation at increasing intraluminal pressures; Figure 3F) and elasticity, as indicated by a lower value of incremental Young's modulus (E_{inc}; Figure 3G). These results suggest aberrant LOX activity contributes to maladaptive venous remodeling. Furthermore, it demonstrates the efficacy of systemic BAPN-mediated inhibition of LOX in improving the biomechanical performance of experimental AVFs.
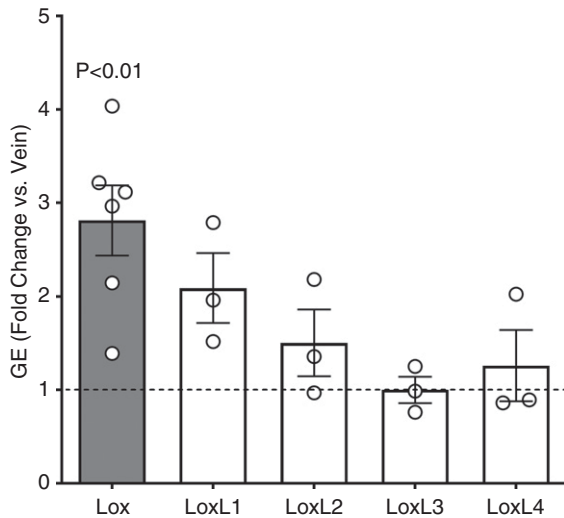
Figure 2. | Lysyl oxidase (LOX) is upregulated in experimental arteriovenous fistulas (AVFs) after surgery. Gene expression (GE) of LOX and LOX-like enzymes (LOXL) in the venous limb of rat AVFs harvested 5 days postsurgery. mRNA expression was normalized with respect to GAPDH and expressed as fold change versus the contralateral vein at the time of AVF creation. Bars represent the mean± SEM, n=3–6 per group.

Scaffold Fabrication and Characterization

We developed an electrospun scaffold that can be applied to the venous adventitia intraoperatively for local, sustained BAPN delivery to the AVF to improve efficacy and minimize off-target effects. After systematic *in vitro* characterization of fabricated scaffolds (data not shown), we identified process (voltage, flow rate, needle diameter, *etc.*) and solution (polymer concentration, drug loading) parameters that yielded fibers with pristine nanoscale morphology and adequate degradation and release kinetics (Figure 4, A and B, Supplemental Figure 5). The average fiber diameter for BAPN and control scaffolds was 185±151 and 392±132 nm (P=0.005), respectively. *In vitro*, both BAPN and control scaffolds degraded entirely in 60 days (Figure 4A). BAPN scaffolds degraded progressively losing 50% of their mass in 30 days, whereas control scaffolds had minimal degradation until day 40. Both scaffolds had degraded beyond detection by day 21 postoperation *in vivo* (data not shown). Drug-loaded scaffolds liberated 20% of BAPN content on day 1 *in vitro*, followed by a progressive release of additional 20% over the next 30 days (Figure 4B).

Local BAPN Delivery Promotes Adaptive Remodeling in Experimental AVFs

We wrapped AVFs intraoperatively with BAPN or vehicle-loaded scaffolds to test the feasibility of local LOX inhibition as prophylactic therapy. BAPN scaffolds significantly decreased wall fibrosis (34.79±3.83 versus 47.17±8.65%, P=0.03) and showed a nonsignificant trend toward higher blood flow compared with controls (34.03±17.32 versus 24.80±7.60 ml/min, P=0.28; Figure 4, C and D) at day 21 postoperation. Of note, irrespective of the presence of drug, the perivascular scaffold modified AVF remodeling in this model, because both groups of animals had higher blood flows and fibrosis compared with the systemic BAPN treatment and control groups (Figure 3, A and C). AVFs wrapped with control scaffolds had more elastin content than those treated with BAPN locally and both systemic experimental groups, suggesting a protective effect of the scaffold on elastin degradation (Supplemental Figure 4B). In contrast to the systemic BAPN treatment, drug-loaded scaffolds significantly decreased elastin deposition, likely as a result of higher effective drug concentrations. Interestingly, there was no significant difference in wall thickness between the local experimental groups, but both showed lower thickness than the systemic control and BAPN arms (Supplemental Figure 3B). Again, these results suggest an effect of the scaffold by itself on AVF remodeling.

As with the systemic treatment (Figure 3, D and E), BAPN decreased immature crosslinking compared with controls (0.82±0.32 versus 1.28±0.29 μmol/mg of dry weight, P=0.03; Figure 4E), and showed a trend toward reduced mature crosslinking (0.07 μmol/mg of dry weight; IQR, 0.05–0.13 versus 0.15; IQR, 0.11–0.38, P=0.07; Figure 4F). Furthermore, consistent with systemic administration of BAPN (Figure 3, F and G), local treatment improved biomechanical properties in the rat AVF model (Figure 4, G and H). These results suggest that local BAPN delivery using perivascular scaffolds is an effective option to improve AVF maturation.

Discussion

We recently established vascular fibrosis as a hallmark of AVF failure (5). However, whether the post-translational modification of newly synthesized collagen determines AVF compliance is uncertain. LOX mediates the oxidation of ε-amino groups of hydroxylysine residues to facilitate crosslinking among collagen bundles (6). Because LOX increases vessel stiffness and reduces elastic compliance in arteries (21,22), we hypothesized that dysregulated LOX activity after AVF creation promotes venous stenosis. Herein, we identified a link between increased LOX deposition in the wall of preaccess human veins and nonmaturation of the AVFs. Collagen was more crosslinked in AVFs that failed than in those achieving maturation. LOX and its ECM substrates were rapidly upregulated after AVF creation in rats. We also demonstrated that systemic and local administration of BAPN reduced collagen crosslinking and promoted adaptive remodeling in rat fistulas. These experiments confirm the noxious effect of LOX during AVF remodeling, paving a new therapeutic avenue to prevent AVF failure.

The higher levels of vascular LOX in human preaccess veins that failed versus those that matured, and of collagen crosslinking in postoperative AVF tissues that failed compared with fistulas that remodeled successfully, suggest that collagen fibrillogenesis is a critical process in determining AVF compliance and outward remodeling early after AVF creation. Despite the self-assembly properties of collagen molecules *in vitro*, collagen fibril formation is heavily regulated in tissues by procollagen N- and C-terminal proteinases, fibronectin, vascular integrins, nonenzymatic collagen glycation, and crosslinking enzymes such as LOX (23,24). Specifically, LOX catalyzes the divalent (immature) bridging of two adjacent collagen triple helices.
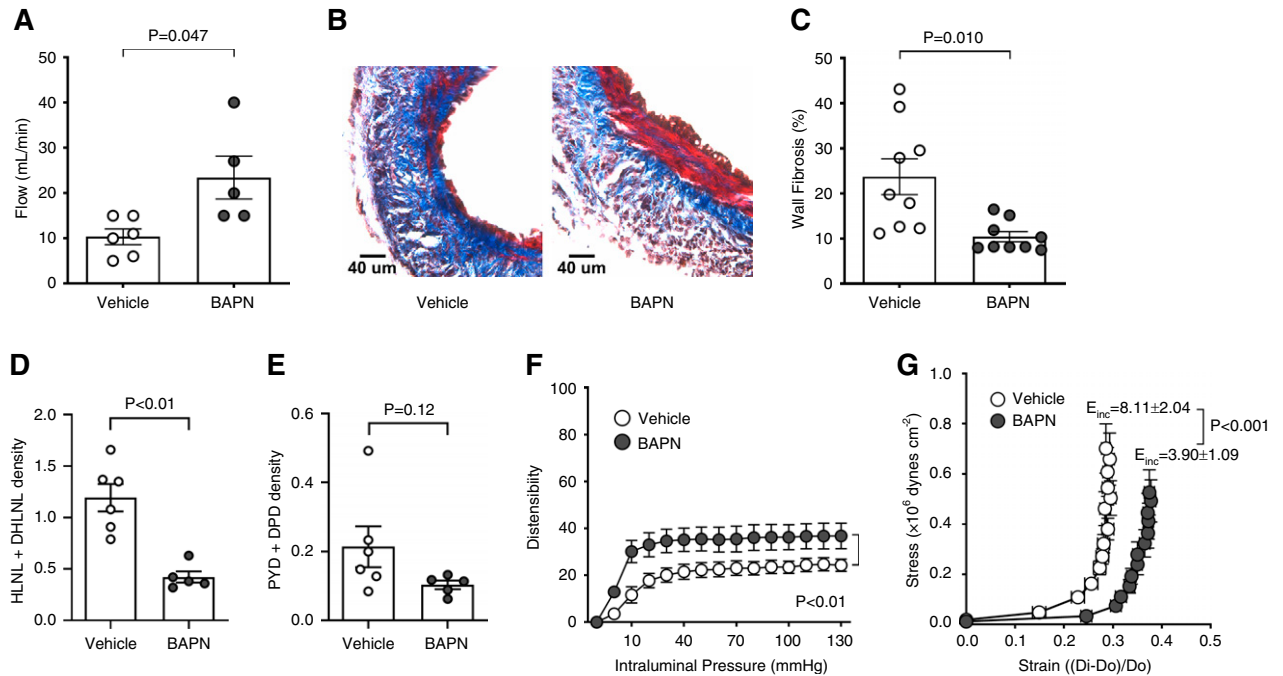
Figure 3. | Systemic inhibition of lysyl oxidase (LOX) with β-aminopropionitrile (BAPN) improves the biomechanical performance of experimental arteriovenous fistulas (AVFs). (A) AVF blood flow in BAPN-treated and control rats at 21 days postsurgery. Bars represent the mean ± SEM ($n=5$–6 per group). (B) Representative Masson's trichrome–stained venous sections from BAPN-treated and control AVFs. Fibrosis stained blue whereas cells are red. (C) Fibrosis quantification (as percent of wall area) in Masson's trichrome–stained sections from both experimental groups. Bars represent the mean±SEM ($n=9$ per group). (D and E) Immature (D) and mature (E) crosslinking density in the venous limb of BAPN-treated and control AVFs as determined by ultra-performance liquid chromatography-electrospray ionization-tandem mass spectrometry (UPLC-ESI-MS/MS; $n=5$–6 per group). Crosslinking density is expressed as μmol per mg of dry weight of tissue. (F and G) AVF distensibility (F) and elasticity (G) assessed in a pressure myograph under Ca^{2+}-free conditions. Distensibility is expressed as percent deformation versus the external diameter of the vein at 3 mm Hg. Elasticity is based on the incremental Young's modulus (E_{inc}), in which lower E_{inc} values are indicative of more elastic vessels. Dots represent the mean±SEM ($n=5$–6 per group).

Within hours, this initial reaction promotes the spontaneous (mature) crosslinking with a third collagen triple helix in a process that continues for months (8). AVFs that failed have significantly higher mature crosslinking than those that matured, and only an increasing trend in immature crosslink density, likely as a result of the continuous modification of collagen fibers during the 2–3 months that elapsed from AVF creation to sample collection. Collagen crosslinking is critical for fibril stability, vascular integrity, and function. However, hyperactive LOX may lead to vascular stiffness, and is known to promote intimal hyperplasia (21,22,25). Our group previously showed that collagen deposition increases significantly after AVF creation in humans, and that increased postoperative medial fibrosis was associated with nonmaturation in a cohort of 115 patients (5). Altogether, the current data suggest that in addition to the degree of postoperative medial fibrosis, collagen crosslinking is an exacerbating factor that contributes to impaired maturation.

Our rat AVF model also demonstrated upregulation of LOX after surgery, along with genes encoding for collagen I and III, the main collagen types involved in vascular remodeling (26,27). Sustained fibronectin upregulation after AVF creation in rats also supports an increase in postoperative fibrillogenesis. These findings are in line with earlier studies, describing increased LOX expression as a requisite for ECM stabilization after arterial injury in rats (28). In the latter

model, elevated LOX activity was associated with acute constrictive remodeling as a result of excessive collagen and elastin crosslinking (28).

We then postulated that inhibition of LOX using BAPN, a natural irreversible inhibitor of LOX (29) and LOXL (14,30), could prove beneficial for postoperative remodeling in the rat AVF model. Systemic BAPN treatment significantly reduced immature crosslinking in AVFs and showed a strong trend toward decreased mature crosslinking. Considering that mature crosslinking of newly synthesized collagen occurs over time, it is possible that a significant change between the control and treatment groups is not detectable at 21 days after AVF creation. Importantly, systemic inhibition of LOX with BAPN during the period of maturation significantly improved the biomechanical performance of AVFs, as indicated by an increase in venous distensibility and elasticity. This increased in elasticity occurred in the absence of changes in elastin content by systemic BAPN, suggesting that elasticity in fistulas is likely more dependent on elastin crosslinking and fiber organization than on protein content. Elastin is not only a substrate of LOX, but its expression is also regulated by LOX at the transcriptional level (31). The role of elastin in AVF remodeling is not clear. Animal models suggest that lower amounts of elastin enhance outward remodeling of the fistula (32). However, a clinical trial with local elastase
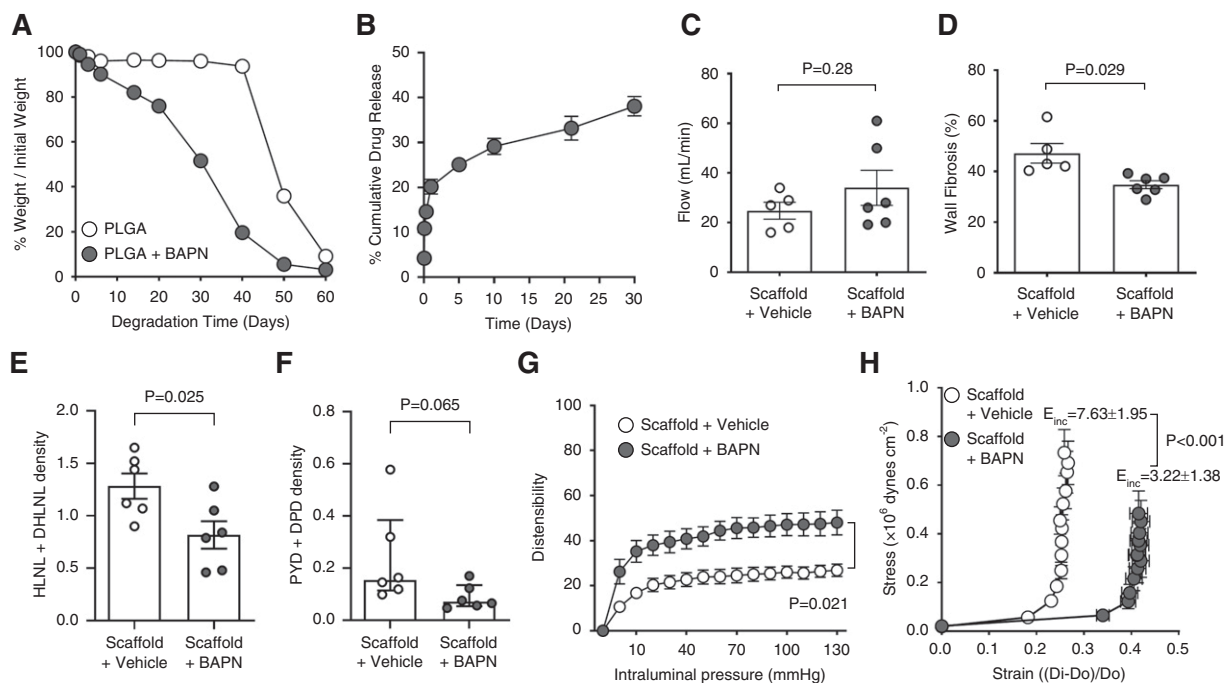
Figure 4. | **Local β-aminopropionitrile (BAPN) delivery improves the biomechanical properties of experimental arteriovenous fistulas (AVFs).** (A) Degradation profiles of BAPN- and vehicle-loaded scaffolds over 60 days *in vitro*. (B) Cumulative BAPN release from PLGA scaffolds over 30 days *in vitro*. (C) AVF blood flow in BAPN-treated and control rats at 21 days postsurgery. Bars represent the mean±SEM (*n*=5–6 per group). (D) Fibrosis quantification (as percent of wall area) in Masson's trichrome–stained venous sections from BAPN-treated and control AVFs. Bars represent the mean±SEM (*n*=5–6 per group). (E and F) Immature (E) and mature (F) crosslinking density in the venous limb of AVFs treated with BAPN and vehicle as quantified by ultra-performance liquid chromatography-electrospray ionization-tandem mass spectrometry (UPLC-ESI-MS/MS; *n*=6 per group). Crosslinking density is expressed as μmol per mg of dry weight. (G and H) AVF distensibility (G) and elasticity (H) assessed in a pressure myograph under Ca^{2+}-free conditions. Distensibility is expressed as percent deformation versus the external diameter of the vein at 3 mm Hg. Elasticity is based on the incremental Young's modulus (E_{inc}), in which lower E_{inc} values are indicative of more elastic vessels. Dots represent the mean ± SEM (*n*=4–6 per group).

improved maturation in radiocephalic AVFs, but not in brachiocephalic fistulas (33).

Electrospun nanofibers have been widely used as vascular biomaterials due to their structural and mechanical properties, which closely resemble the vascular ECM (34–37). We developed an electrospun scaffold for perivascular delivery of BAPN to increase the effective drug concentration while minimizing off-target effects (38). BAPN-loaded nanofibers progressively eroded over 60 days *in vitro*, whereas control scaffolds had negligible mass loss until day 40, consistent with bulk degradation (39). BAPN scaffolds had a biphasic drug release profile with a drastic burst followed by sustained release. Surface erosion and burst release of BAPN scaffolds can be attributed to the presence of the hydrophilic BAPN at the fiber interface, which facilitates hydrolysis at the fiber surface and early release (39–42). This pharmacokinetic profile was effective at decreasing immature crosslinking and fibrosis, and improving biomechanical properties, in agreement with the systemic BAPN regimen. However, further characterization of the effects of PLGA scaffolds on AVF remodeling is needed, because both scaffold treatment groups had higher fibrosis and blood flow than the systemic arms, despite similar crosslinking and biomechanical properties between the corresponding drug-to-drug and vehicle-to-vehicle comparisons. In fact, control scaffolds resulted in higher elastin

content than drug-loaded scaffolds and both systemic experimental groups, suggesting a protective effect of the empty scaffold on elastin degradation. Unlike the systemic treatment, the higher effective drug concentration achieved with local BAPN delivery decreased elastin content in the drug-loaded group, in agreement with published studies in which BAPN annulled the positive action of LOX on the elastin promoter (31). Despite less elastin, AVFs treated with drug-loaded scaffolds had higher elasticity than controls, again indicating that elasticity in fistulas in dependent on other factors besides elastin content. Another interesting effect observed in both scaffold treatment groups was reduced AVF wall thickness with respect to the systemic experimental arms. This effect may explain the higher blood flows observed compared with the latter, and is in line with published work with drug-free PLGA scaffolds in porcine vein grafts (43,44). Overall, our results suggest that periadventitial scaffolds alter adaptive remodeling *via* multiple mechanisms, including a potential contribution of "external stenting" (44–50). It has been proposed that bioabsorbable, nonrestrictive scaffolds improve vein remodeling by (*1*) modulating hemodynamic forces, (2) increasing vascularization of the adventitia, and/or (3) promoting outward migration (as opposed to inward remodeling) of smooth muscle cells in response to inflammatory cell infiltration of the scaffold (51).

One question that remains is whether the different types of collagen crosslinks play distinct roles in AVF remodeling. It would be difficult to separate their effects because mature crosslinks depend on the occurrence of immature ones. However, it is tempting to hypothesize that mature crosslinks are more restrictive for AVF biomechanics given their interactions with a third collagen triple helix. In contrast, different levels of collagen organization may have distinct effects on *de novo* collagen deposition, binding of LOX and other ECM-remodeling enzymes, sequestration of growth factors, migration of cells, *etc*. Inhibition of immature crosslinks was sufficient to improve biomechanics in the rat AVF without significantly changing mature crosslinking. Future studies where AVF biomechanics are studied at increasing time points after creation may allow for a better evaluation of the roles of mature versus immature crosslinking in remodeling.

The limitations of the study include the use of a small animal model for investigating AVF hemodynamics, the lack of specificity of BAPN, which also targets LOXL enzymes (29,52–56), the lack of statistical power to evaluate sex-related effects, and the use of a nonunidirectional scaffold that allows drug release to perivascular tissues. Addressing these limitations in the future may prove instrumental to the development of novel preventive therapies for early AVF failure. Despite these issues, we demonstrated the efficacy of systemic and perivascular BAPN-mediated inhibition of LOX in improving the biomechanical properties of experimental AVFs. Given the observed differences in collagen crosslinking between human AVFs that failed and those that matured, our results advocate that inhibition of LOX is an effective method to optimize outward remodeling after AVF creation.

Disclosures

Funding

Author Contributions

Supplemental Material

This article contains the following supplemental material online at http://kidney360.asnjournals.org/lookup/suppl/doi:10.34067/KID.K3602020000501/-/DCSupplemental.

Supplemental Materials and Methods.

Supplemental References.

Supplemental Figure 1. Postoperative venous remodeling and LOX localization in the rat femoral-epigastric AVF.

Supplemental Figure 2. Postoperative gene expression (GE) of vascular remodeling genes in the venous limb of the rat femoral-epigastric AVF.

Supplemental Figure 3. Fibrosis and wall thickness in BAPN-treated and control AVFs.

Supplemental Figure 4. Elastin content in BAPN-treated and control AVFs.

Supplemental Figure 5. Scanning electron microphotograph of BAPN-loaded PLGA nanofibers.

References

1. National Kidney Foundation: KDOQI clinical practice guideline for hemodialysis adequacy: 2015 update [published correction appears in Am J Kidney Dis 67: 534, 2016]. *Am J Kidney Dis* 66: 884–930, 2015 https://doi.org/10.1053/j.ajkd.2015.07.015
2. Konner K, Nonnast-Daniel B, Ritz E: The arteriovenous fistula. *J Am Soc Nephrol* 14: 1669–1680, 2003 https://doi.org/10.1097/01.ASN.0000069219.88168.39
3. Robbin ML, Greene T, Cheung AK, Allon M, Berceli SA, Kaufman JS, Allen M, Imrey PB, Radeva MK, Shiu YT, Umphrey HR, Young CJ; Hemodialysis Fistula Maturation Study Group: Arteriovenous fistula development in the first 6 weeks after creation. *Radiology* 279: 620–629, 2016 https://doi.org/10.1148/radiol.2015150385
4. Al-Jaishi AA, Oliver MJ, Thomas SM, Lok CE, Zhang JC, Garg AX, Kosa SD, Quinn RR, Moist LM: Patency rates of the arteriovenous fistula for hemodialysis: A systematic review and meta-analysis. *Am J Kidney Dis* 63: 464–478, 2014 https://doi.org/10.1053/j.ajkd.2013.08.023
5. Martinez L, Duque JC, Tabbara M, Paez A, Selman G, Hernandez DR, Sundberg CA, Tey JCS, Shiu YT, Cheung AK, Allon M, Velazquez OC, Salman LH, Vazquez-Padron RI: Fibrotic venous remodeling and nonmaturation of arteriovenous fistulas. *J Am Soc Nephrol* 29: 1030–1040, 2018 https://doi.org/10.1681/ASN.2017050559
6. Siegel RC: Lysyl oxidase. *Int Rev Connect Tissue Res* 8: 73–118, 1979 https://doi.org/10.1016/B978-0-12-363708-6.50009-6
7. Rodríguez C, Rodríguez-Sinovas A, Martínez-González J: Lysyl oxidase as a potential therapeutic target. *Drug News Perspect* 21: 218–224, 2008 https://doi.org/10.1358/dnp.2008.21.4.1213351
8. Rodriguez-Pascual F, Slatter DA: Collagen cross-linking: Insights on the evolution of metazoan extracellular matrix. *Sci Rep* 6: 37374, 2016 https://doi.org/10.1038/srep37374

9. Wagenseil JE, Mecham RP: New insights into elastic fiber assembly. *Birth Defects Res C Embryo Today* 81: 229–240, 2007 https://doi.org/10.1002/bdrc.20111

10. Johnston KA, Lopez KM: Lysyl oxidase in cancer inhibition and metastasis. *Cancer Lett* 417: 174–181, 2018 https://doi.org/10.1016/j.canlet.2018.01.006

11. Erler JT, Giaccia AJ: Lysyl oxidase mediates hypoxic control of metastasis. *Cancer Res* 66: 10238–10241, 2006 https://doi.org/10.1158/0008-5472.CAN-06-3197

12. López B, González A, Hermida N, Valencia F, de Teresa E, Díez J: Role of lysyl oxidase in myocardial fibrosis: From basic science to clinical aspects. *Am J Physiol Heart Circ Physiol* 299: H1–H9, 2010 https://doi.org/10.1152/ajpheart.00335.2010

13. Nave AH, Mižíková I, Niess G, Steenbock H, Reichenberger F, Talavera ML, Veit F, Herold S, Mayer K, Vadász I, Weissmann N, Seeger W, Brinckmann J, Morty RE: Lysyl oxidases play a causal role in vascular remodeling in clinical and experimental pulmonary arterial hypertension. *Arterioscler Thromb Vasc Biol* 34: 1446–1458, 2014 https://doi.org/10.1161/ATVBAHA.114.303534

14. Peacock EE, Madden JW: Administration of beta-aminopropionitrile to human beings with urethral strictures: A preliminary report. *Am J Surg* 136: 600–605, 1978 https://doi.org/10.1016/0002-9610(78)90317-3

15. Keiser HR, Sjoerdsma A: Studies on beta-aminopropionitrile in patients with scleroderma. *Clin Pharmacol Ther* 8: 593–602, 1967 https://doi.org/10.1002/cpt196784593

16. Globerman AS, Chaouat M, Shlomai Z, Galun E, Zeira E, Zamir G: Efficient transgene expression from naked DNA delivered into an arterio-venous fistula model for kidney dialysis. *J Gene Med* 13: 611–621, 2011 https://doi.org/10.1002/jgm.1615

17. Machon C, Le Calve B, Coste S, Riviere M, Payen L, Bernard D, Guitton J: Quantification of β-aminopropionitrile, an inhibitor of lysyl oxidase activity, in plasma and tumor of mice by liquid chromatography tandem mass spectrometry. *Biomed Chromatogr* 28: 1017–1023, 2014 https://doi.org/10.1002/bmc.3110

18. Hernandez DR, Del Carmen Piqueras M, Macias AE, Martinez L, Vazquez-Padron R, Bhattacharya SK: Immature and mature collagen crosslinks quantification using high-performance liquid chromatography and high-resolution mass spectrometry in orbitrap™. *Methods Mol Biol* 1996: 101–111, 2019 https://doi.org/10.1007/978-1-4939-9488-5_10

19. Briones AM, Salaices M, Vila E: Mechanisms underlying hypertrophic remodeling and increased stiffness of mesenteric resistance arteries from aged rats. *J Gerontol A Biol Sci Med Sci* 62: 696–706, 2007 https://doi.org/10.1093/gerona/62.7.696

20. Martinez L, Tabbara M, Duque JC, Selman G, Falcon NS, Paez A, Griswold AJ, Ramos-Echazabal G, Hernandez DR, Velazquez OC, Salman LH, Vazquez-Padron RI: Transcriptomics of human arteriovenous fistula failure: Genes associated with non-maturation. *Am J Kidney Dis* 74: 73–81, 2019 https://doi.org/10.1053/j.ajkd.2018.12.035

21. Eberson LS, Sanchez PA, Majeed BA, Tawinwung S, Secomb TW, Larson DF: Effect of lysyl oxidase inhibition on angiotensin II-induced arterial hypertension, remodeling, and stiffness. *PLoS One* 10: e0124013, 2015 https://doi.org/10.1371/journal.pone.0124013

22. Martínez-Revelles S, García-Redondo AB, Avendaño MS, Varona S, Palao T, Orriols M, Roque FR, Fortuño A, Touyz RM, Martínez-González J, Salaices M, Rodríguez C, Briones AM: Lysyl oxidase induces vascular oxidative stress and contributes to arterial stiffness and abnormal elastin structure in hypertension: Role of p38MAPK. *Antioxid Redox Signal* 27: 379–397, 2017 https://doi.org/10.1089/ars.2016.6642

23. Sorushanova A, Delgado LM, Wu Z, Shologu N, Kshirsagar A, Raghunath R, Mullen AM, Bayon Y, Pandit A, Raghunath M, Zeugolis DI: The collagen suprafamily: From biosynthesis to advanced biomaterial development. *Adv Mater* 31: e1801651, 2019 https://doi.org/10.1002/adma.201801651

24. Kadler KE, Hill A, Canty-Laird EG: Collagen fibrillogenesis: Fibronectin, integrins, and minor collagens as organizers and nucleators. *Curr Opin Cell Biol* 20: 495–501, 2008 https://doi.org/10.1016/j.ceb.2008.06.008

25. Rodríguez M, Pascual G, Cifuentes A, Perez-Köhler B, Bellón JM, Buján J: Role of lysyl oxidases in neointima development in vascular allografts. *J Vasc Res* 48: 43–51, 2011 https://doi.org/10.1159/000317399

26. Hall MR, Yamamoto K, Protack CD, Tsuneki M, Kuwahara G, Assi R, Brownson KE, Bai H, Madri JA, Dardik A: Temporal regulation of venous extracellular matrix components during arteriovenous fistula maturation. *J Vasc Access* 16: 93–106, 2015 https://doi.org/10.5301/jva.5000290

27. Wagenseil JE, Mecham RP: Vascular extracellular matrix and arterial mechanics. *Physiol Rev* 89: 957–989, 2009 https://doi.org/10.1152/physrev.00041.2008

28. Nuthakki VK, Fleser PS, Malinzak LE, Seymour ML, Callahan RE, Bendick PJ, Zelenock GB, Shanley CJ: Lysyl oxidase expression in a rat model of arterial balloon injury. *J Vasc Surg* 40: 123–129, 2004 https://doi.org/10.1016/j.jvs.2004.02.028

29. Tang SS, Trackman PC, Kagan HM: Reaction of aortic lysyl oxidase with beta-aminopropionitrile. *J Biol Chem* 258: 4331–4338, 1983

30. Peacock EE Jr, Madden JW: Some studies on the effects of beta-aminopropionitrile in patients with injured flexor tendons. *Surgery* 66: 215–223, 1969

31. Oleggini R, Gastaldo N, Di Donato A: Regulation of elastin promoter by lysyl oxidase and growth factors: Cross control of lysyl oxidase on TGF-beta1 effects. *Matrix Biol* 26: 494–505, 2007 https://doi.org/10.1016/j.matbio.2007.02.003

32. Wong CY, Rothuizen TC, de Vries MR, Rabelink TJ, Hamming JF, van Zonneveld AJ, Quax PH, Rotmans JI: Elastin is a key regulator of outward remodeling in arteriovenous fistulas. *Eur J Vasc Endovasc Surg* 49: 480–486, 2015 https://doi.org/10.1016/j.ejvs.2014.12.035

33. Hye RJ, Peden EK, O'Connor TP, Browne BJ, Dixon BS, Schanzer AS, Jensik SC, Dember LM, Jaff MR, Burke SK: Human type I pancreatic elastase treatment of arteriovenous fistulas in patients with chronic kidney disease. *J Vasc Surg* 60: 454–461.e1, 2014 https://doi.org/10.1016/j.jvs.2014.02.037

34. Chen X, Wang J, An Q, Li D, Liu P, Zhu W, Mo X: Electrospun poly(L-lactic acid-co--caprolactone) fibers loaded with heparin and vascular endothelial growth factor to improve blood compatibility and endothelial progenitor cell proliferation. *Colloids Surf B Biointerfaces* 128: 106–114, 2015 https://doi.org/10.1016/j.colsurfb.2015.02.023

35. Kennedy KM, Bhaw-Luximon A, Jhurry D: Cell-matrix mechanical interaction in electrospun polymeric scaffolds for tissue engineering: Implications for scaffold design and performance. *Acta Biomater* 50: 41–55, 2017 https://doi.org/10.1016/j.actbio.2016.12.034

36. Repanas A, Andriopoulou S, Glasmacher B: The significance of electrospinning as a method to create fibrous scaffolds for biomedical engineering and drug delivery applications. *J Drug Deliv Sci Technol* 31: 137–146, 2016 https://doi.org/10.1016/j.jddst.2015.12.007

37. Wen M, Zhi D, Wang L, Cui C, Huang Z, Zhao Y, Wang K, Kong D, Yuan X: Local delivery of dual microRNAs in trilayered electrospun grafts for vascular regeneration. *ACS Appl Mater Interfaces* 12: 6863–6875, 2020 https://doi.org/10.1021/acsami.9b19452

38. Barrow MV, Simpson CF: Caution against the use of lathyrogens. *Surgery* 71: 309–310, 1972

39. Göpferich A: Mechanisms of polymer degradation and erosion. *Biomaterials* 17: 103–114, 1996 https://doi.org/10.1016/0142-9612(96)85755-3

40. Heller J: Controlled release of biologically active compounds from bioerodible polymers. *Biomaterials* 1: 51–57, 1980 https://doi.org/10.1016/0142-9612(80)90060-5

41. Makadia HK, Siegel SJ: Poly Lactic-co-Glycolic Acid (PLGA) as biodegradable controlled drug delivery carrier. *Polymers (Basel)* 3: 1377–1397, 2011 https://doi.org/10.3390/polym3031377

42. Pitt CG, Gratzl MM, Kimmel GL, Surles J, Schindler A: Aliphatic polyesters II. The degradation of poly (DL-lactide), poly (ε-caprolactone), and their copolymers in vivo. *Biomaterials* 2: 215–220, 1981 https://doi.org/10.1016/0142-9612(81)90060-0

43. Vijayan V, Shukla N, Johnson JL, Gadsdon P, Angelini GD, Smith FC, Baird R, Jeremy JY: Long-term reduction of medial and intimal thickening in porcine saphenous vein grafts with a polyglactin biodegradable external sheath. *J Vasc Surg* 40: 1011–1019, 2004 https://doi.org/10.1016/j.jvs.2004.08.047

44. Jeremy JY, Bulbulia R, Johnson JL, Gadsdon P, Vijayan V, Shukla N, Smith FC, Angelini GD: A bioabsorbable (polyglactin), non-restrictive, external sheath inhibits porcine saphenous vein graft thickening. *J Thorac Cardiovasc Surg* 127: 1766–1772, 2004 https://doi.org/10.1016/j.jtcvs.2003.09.054

45. Xie P, Shi E, Gu T, Zhang Y, Mao N: Inhibition of intimal hyperplasia of the vein graft with degradable poly lactic-co-glycolic acid vascular external sheaths carrying slow-release bosentan. *Eur J Cardiothorac Surg* 48: 842–849; discussion 849, 2015 https://doi.org/10.1093/ejcts/ezv025

46. Mylonaki I, Trosi O, Allémann E, Durand M, Jordan O, Delie F: Design and characterization of a perivascular PLGA coated PET mesh sustaining the release of atorvastatin for the prevention of intimal hyperplasia. *Int J Pharm* 537: 40–47, 2018 https://doi.org/10.1016/j.ijpharm.2017.12.026

47. Izzat MB, Mehta D, Bryan AJ, Reeves B, Newby AC, Angelini GD: Influence of external stent size on early medial and neointimal thickening in a pig model of saphenous vein bypass grafting. *Circulation* 94: 1741–1745, 1996 https://doi.org/10.1161/01.CIR.94.7.1741

48. George SJ, Izzat MB, Gadsdon P, Johnson JL, Yim APC, Wan S, Newby AC, Angelini GD, Jeremy JY: Macro-porosity is necessary for the reduction of neointimal and medial thickening by external stenting of porcine saphenous vein bypass grafts. *Atherosclerosis* 155: 329–336, 2001 https://doi.org/10.1016/S0021-9150(00)00588-8

49. Mehta D, George SJ, Jeremy JY, Izzat MB, Southgate KM, Bryan AJ, Newby AC, Angelini GD: External stenting reduces long-term medial and neointimal thickening and platelet derived growth factor expression in a pig model of arteriovenous bypass grafting. *Nat Med* 4: 235–239, 1998 https://doi.org/10.1038/nm0298-235

50. Ben-Gal Y, Taggart DP, Williams MR, Orion E, Uretzky G, Shofti R, Banai S, Yosef L, Bolotin G: Expandable external support device to improve Saphenous Vein Graft Patency after CABG. *J Cardiothorac Surg* 8: 122, 2013 https://doi.org/10.1186/1749-8090-8-122

51. Desai M, Mirzay-Razzaz J, von Delft D, Sarkar S, Hamilton G, Seifalian AM: Inhibition of neointimal formation and hyperplasia in vein grafts by external stent/sheath. *Vasc Med* 15: 287–297, 2010 https://doi.org/10.1177/1358863X10366479

52. Nilsson M, Adamo H, Bergh A, Halin Bergström S: Inhibition of lysyl oxidase and lysyl oxidase-like enzymes has tumour-promoting and tumour-suppressing roles in experimental prostate cancer. *Sci Rep* 6: 19608, 2016 https://doi.org/10.1038/srep19608

53. Jung ST, Kim MS, Seo JY, Kim HC, Kim Y: Purification of enzymatically active human lysyl oxidase and lysyl oxidase-like protein from Escherichia coli inclusion bodies. *Protein Expr Purif* 31: 240–246, 2003 https://doi.org/10.1016/S1046-5928(03)00217-1

54. Kim MS, Kim SS, Jung ST, Park JY, Yoo HW, Ko J, Csiszar K, Choi SY, Kim Y: Expression and purification of enzymatically active forms of the human lysyl oxidase-like protein 4. *J Biol Chem* 278: 52071–52074, 2003 https://doi.org/10.1074/jbc.M308856200

55. Lee JE, Kim Y: A tissue-specific variant of the human lysyl oxidase-like protein 3 (LOXL3) functions as an amine oxidase with substrate specificity. *J Biol Chem* 281: 37282–37290, 2006 https://doi.org/10.1074/jbc.M600977200

56. Rodriguez HM, Vaysberg M, Mikels A, McCauley S, Velayo AC, Garcia C, Smith V: Modulation of lysyl oxidase-like 2 enzymatic activity by an allosteric antibody inhibitor. *J Biol Chem* 285: 20964–20974, 2010 https://doi.org/10.1074/jbc.M109.094136